Molecular BioSystems

Accepted Manuscript

This article can be cited before page numbers have been issued, to do this please use: Y. Pu, S. Zhang, Z. chang, Y. Zhang, D. wang, L. zhang, Y. Li and Z. Zuo, *Mol. BioSyst.*, 2016, DOI: 10.1039/C6MB00712K.

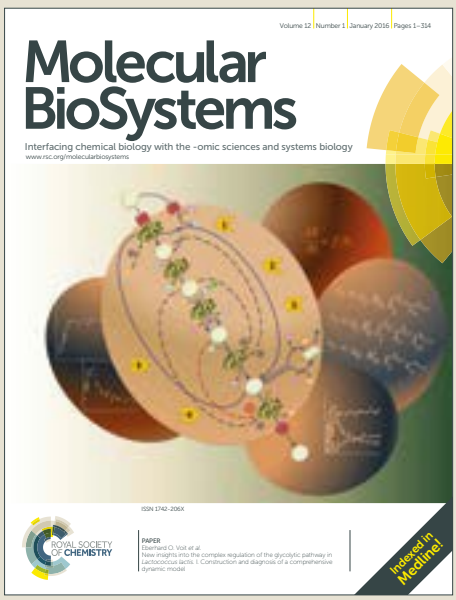

This is an Accepted Manuscript, which has been through the Royal Society of Chemistry peer review process and has been accepted for publication.

Accepted Manuscripts are published online shortly after acceptance, before technical editing, formatting and proof reading. Using this free service, authors can make their results available to the community, in citable form, before we publish the edited article. We will replace this Accepted Manuscript with the edited and formatted Advance Article as soon as it is available.

You can find more information about Accepted Manuscripts in the author guidelines.

Please note that technical editing may introduce minor changes to the text and/or graphics, which may alter content. The journal's standard Terms & Conditions and the ethical guidelines, outlined in our author and reviewer resource centre, still apply. In no event shall the Royal Society of Chemistry be held responsible for any errors or omissions in this Accepted Manuscript or any consequences arising from the use of any information it contains.

ROYAL SOCIETY OF CHEMISTRY

rsc.li/molecular-biosystems

View Article Online
DOI: 10.1039/C6MB00712K

Discovery of new dual binding TNKS inhibitors of Wnt Signaling Inhibition by pharmacophore modeling, molecular docking and bioassay

Yinglan Pu[a,b], Shuqun Zhang[b], Zhe Chang[b], Yunqin Zhang[b], Dong Wang[b], Li Zhang[a]*, Yan Li [b,c]*, Zhili Zuo[b,c]*

[a]School of Chemical Engineering, Sichuan University of Science & Engineering, Zigong, China

[b]State Key Laboratory of Phytochemistry and Plant Resources in West China, Kunming Institute of Botany, Chinese Academy of Sciences, Kunming, China

[c]Yunnan Key Laboratory of Natural Medicinal Chemistry

* Corresponding author: Zhili Zuo, Li Zhang, Yan Li, Tel./Fax: +86-871-65227196

E-Mail: zuozhili@mail.kib.ac.cn

ABSTRACT: Tankyrases（TNKS）, key transmitters in the Wnt signal pathway which is very conservative in the evolution, are vital targets as they are over expressed widely in many cancers. In this work, 5 inhibitors with novel structures have been discovered and validated using the ligand-based (pharmacophore) virtual screening, docking study, and Luciferase reporter assays of Wnt signaling. Among them, **PYL-1**, particularly, was the most potent inhibitor with IC_{50} value of 9.56μM against Wnt signaling. The analysis of binding modes was performed to further understand the vital interactions between inhibitors and TNKS 2, and the five hits belong to dual sites inhibitors. This work could be helpful in design and development of novel dual binders as TNKS inhibitors.

Key words: TNKS, Wnt signal pathway, cancers, pharmacophore, docking study

1. Introduction

Wnt signal pathway, a very conservative pathway in the evolution, is widely

View Article Online
DOI: 10.1039/C6MB00712K

activated in many cancers so that it usually has a close relationship with tumors.[1, 2] TNKS can increase β-catenin by reducing the expression of Axis to make Wnt signal pathway raise,[3, 4] which is overexpressed in the majority of tumors. Meanwhile TNKS act as members of adenosine diphosphate ribose polymerase (PARP) family and have an important influence on the length of telomere.[5, 6] TNKS can let the length of telomere increase by ribosylating of telomeric protein TRF1 to make normal cell divide excessively and cancerate.[7-9] In addition, TNKS also play an important role in the mitosis. TNKS1 binds to NuMA (nuclear mitotic apparatus protein) to form an essential compound protein for mitotic spindle assembly and stabilization.[10, 11] It`s shown that TNKS inhibition could also disturb the rapid growth of cancer cells.[12, 13] Therefore, blocking of TNKS has been regarded as a promising and effective therapeutic approach against a variety of cancers.[14, 15]

TNKS are members of the poly(ADP ribose) polymerase (PARP) protein superfamily containing 18 members. TNKS have two subtypes: TNKS1 and TNKS2 , which are also named as ARTD5 (PARP-5a) and ARTD6 (PARP-5b), respectively.[16, 17] TNKS 1 overlaps lots of functions of TNKS 2.[18, 19]They have three vital roles in telomere homeostasis, in mitosis, and in Wnt signaling. Once these processes disorder, many diseases will occur such as kinds of cancers. Therefore, discovering of novel TNKS inhibitors is in urgent need in the treatment of cancers.[20, 21]

However, all promising TNKS inhibitors are still in the theoretical study.[22] Some structurally diverse inhibitors of TNKS include three sorts of binding sites: XAV939[3] binds the well-known canonical PARP pharmacophore working as nicotinamide isosteres;[23] JW55[24] and IWR1/IWR2[25, 26]bind to the adjacent induced pocket; 3-((4-oxo-3,4-dihydroquinazolin-2-yl)thio) propanamides derivatives[27] belong to dual binders. Furthermore, drugs binding a single active site have limited clinical efficacy for a highly complex, multifactorial disease such as cancer. Dual sites drugs may have therapeutic effects. Although many TNKS hits binding to a single active site are still being found, so far the novel double-site inhibitors have a limited number. Hence, discovering of novel TNKS dual sites inhibitors is attractive for cancer therapy.

View Article Online
DOI: 10.1039/C6MB00712K

As all known, research and development of new drug is high input, high-tech content, high competition, high-income activities, it has a wide range of links, spend more money, long R & D cycle, the success rate is low, the system is complex and so on.[28] Therefore, computer-aided drug design (CADD) appears to become increasingly important to accelerate the drug discovery process. CADD can be divided into two types, receptor based and ligand based drug design.[29] In this study, to shorten the new drug development cycle and reduce the costs, receptor based virtual screening (docking) and ligand-based screening (HipHop pharmacophore) were performed. The molecular docking was firstly used to refine the specs compounds that filtered by Rule of five and Veber rules. The pharmacophore features, which were based on known TNKS inhibitors, were used to query new potent inhibitors.[30] The best pharmacophore hypothese (Hypo 1) was then used for screening the remain top 10000 molecules according to docking score list (**Figure 1**). Eventually, 13 active inhibitors obtained from virtual screening were further evaluated by in vitro biological tests on HEK293T cells.

2 Materials and methods

2.1 Methods and computational details

Docking and pharmacophore using the specs database were applied to identify novel potential TNKS inhibitors. Pharmacophore-based screening was carried out using Discovery Studio Version 4.0 (DS 4.0, Accelrys Inc., San Diego, CA) and molecular docking studies were performed using GOLD 5.2.2(Genetic Optimization of Ligand Docking). Pharmacophore module of DS 4.0 was used to generate pharmacophore models of TNKS inhibitors and search for the potential inhibitors. The working flow chart for this study, including ligand-based (HipHop pharmacophore) screening and molecular docking, is illustrated in **Figure 1**.

2.2 Data preparation

Five types of duel sites TNKS 2 inhibitors were collected from 5 publications as training set to generate common features in pharmacophore models, including

View Article Online
DOI: 10.1039/C6MB00712K

WIKI4[31], UHB[32], Olaparib[33], **49**[27], **4**[34](**Figure 2**). 5 structural diverse compounds with IC_{50} values ranged from 0.001nM to 0.002μM were selected as the training set; while the test set contained 34 active molecules (the analogues of **49**) [27] and 54 inactive molecules were collected according to the method described by Yang.[35] At first, we selected the compounds with identity of less than 60 percent of the active molecules from Zink database (http://zinc.docking.org). And then 54 molecules with the most similar molecular properties of training set were selected. All the molecules were prepared and optimized using DS 4.0.

The X-ray crystal structure of TNKS 2 (PDB ID: 3U9Y), which complexed with Olaparib, having 2.3 Å resolution, was considered for this study. The obtained protein was firstly prepared by removing water molecules and some other co-crystallized small molecules in the system with DS 4.0. Then hydrogen was added and the whole structure was optimized with SYBYL-X 2.0 (SYBYL). The prepared protein was later used for docking.

2.3 Molecular Docking

The specs database, which consists of about 220000 small molecules, was exposed to virtual screening. These compounds were downloaded from specs official website (www.specs.net) and optimized via DS 4.0.

At first, all these compounds were filtered by the Lipinski's "Rule of five" and Veber rules, which were widely used in the early stage discovery of new drugs. According to the rules, we can eliminate numerous molecules with poor drug-like properties and low ADMET abilities, such as breaking "Rule of five": molecule weight more than 500 Daltons, more than 5 hydrogen bond donors, more than 10 hydrogen bond acceptors, and octanol-water partition coefficient logP greater than 5.[36] And straying from Veber rules: more than 10 rotatable bonds and polar surface area equal to or more than 140 $Å^2$ (or more than 12 H-bond donors and acceptors).[37] Therefore, 75671 molecules were remained to treat as docking library into the TNKS-2 crystal structure.

View Article Online
DOI: 10.1039/C6MB00712K

The molecular docking in this study was carried out with GOLD[38]. Before screening, we've tried a variety of scoring functions to obtain the optimal parameters. Among them, when the inner-ligand (Olaparib) was re-docked into the binding pocket with the scoring function of Chemplp, the root mean square deviation (RMSD) of all atoms between docked pose and original conformation was minimum (0.528Å). Chemplp was then used for the further study. The active pocket was defined by a grid with outer box dimensions of 8Å centered with the ligand. Each molecule was docked 30 times. Other docking operations were performed with the default settings.

2.4 HipHop Pharmacophore model

The DS 4.0 was used for the preparation of protein, generation of pharmacophore and validation in this study. And the HipHop algorithm was used for ligand-based pharmacophore modelling. On the first step: the preparation of training set. Three criteria were complied with to build HipHop model： structurally diverse representatives；2 to 32 inhibitors; high bioactivity. Based on the above three criteria, 5 TNKS 2 inhibitors were selected as training set. The parameters were set as follows. The Principal and MaxOmitFeat attributes were defined as highly active and matching all characteristic elements, the values were 2 and 0, respectively. On the second step, the Pharmacophore characteristic elements were selected by visual inspection and through Feature Mapping tool. The Details of results showed training set contained the sorts and number of common features which were the base of the third step. The feature elements was extracted based on structural features and activity. The five compounds in the training set contained 6 features of HB-ACCEPTOR, HB_ACCEPTOR_lipid, RING_AROMATIC, HBA_HEAVY, HBA_PROJECTION, HBD_1, which were chosen to generate the common feature pharmacophore. Among them ， HB-ACCEPTOR represents Hydrogen-Bonding Acceptor, HB_ACCEPTOR_lipid represents lipidic hydrogen bond acceptor, RING_AROMATIC represents ring aromatic, HBA_HEAVY represents the heavy

View Article Online
DOI: 10.1039/C6MB00712K

atom of a hydrogen bond acceptor, HBA_PROJECTION represents the projection point of a hydrogen bond acceptor, and HBD_1 represented hydrogen bond donor and matching an aromatic carbon with a hydrogen. And the all of Minimum and Maximum Features parameter of each was respectively set as 0 and 5. The BEST option was used to generate the conformations, using the maximum limit of 200 conformations within a 10 kcal/mol cutoff. The rests of the parameters were set at default values.

10 hypotheses (Hypo) were generated with different combination of features and scores. 34 active molecules and 54 inactive molecules were considered as test set compounds for the validation. The main purpose of this validation was to pick out the most suitable Hypo from the ten pharmacophore models. Eventually Hypo 1 turned out to be the best pharmacophore, which was selected for further studies, based on the good-fit values, heat map(**Figure 3**) and the interaction points available at the active site.

2.5 Virtual screening

Hypo 1, appeared to be the best pharmacophore model, was used to screen the top 10000 compounds in the docking score list. Most of parameters were set to the default and the Number of Conformations was set to 200, the Conformation Method was set to BEST. While Minimum Interfeature Distance was set to 2, Limit Hits was set to First N, Maximum Hits was set to 500. Therefore, the top 500 molecules were used cluster analysis to further screen.

2.6 Cluster analysis

After the pharmacophore-based screening, the top-ranked 500 molecules were retained for further cluster analysis, visual inspection of binding mode and the ligand fitness of the pharmacophore. Finally, 13 compounds, which have structural diversity, proper binding modes and good fitness, were considered as fit conformation. Therefore, they were selected and purchased from specs company to detect their

View Article Online
DOI: 10.1039/C6MB00712K

bioactivities.

2.7 Luciferase reporter assay of transcriptional activity of wnt signaling

As a key transmitter in the Wnt signaling path way, the activity of TNKS must correlate with the strength of the signal. Luciferase reporter assays of Wnt signaling were thus used to test the potency against TNKS. Luciferase reporter assays of Wnt signaling were done in 96-well plates with three repeats. HEK293T cells were seeded in 96-well plates for overnight culture. Then cells were cotransfected with 80 ng of Wnt/β-catenin signaling responsive Firefly luciferase reporter plasmid SuperTOPflash, 8 ng of Renilla reporter plasmid and 64ng of Wnt1. After 3 h incubation, cells were exposed to various concentrations of test chemicals for 24 h and then the cells were lysed. Luciferase activities were measured using the Dual-Luciferase Reporter Assay kit (Promega, Madison, WI). Topflash luciferase activities were normalized to the Renilla activities.

3 Result and discussion

3.1 Molecular Docking

Docking simulation of TNKS 2 was performed using the protocol of GOLD. The specs database was first filtered by Lipinski's "Rule of five" and Veber rules. Eventually, 75671 compounds were remained to be used Molecular Docking. Top 10000 compounds of scoring list were preserved for the virtual screening.

3.2 Pharmacophore Generation and validation

HipHop algorithm, which is based on the common features present in the training set molecules, was applied to further screen the molecular docking results. Before the start of pharmacophore modeling, we collected 5 TNKS 2 inhibitors binding to dual sites from different literature resources to form a training set based on good activities and structural diversity. Structures of the training set compounds were shown in **Figure 2**. Ten hypotheses were mainly composed of two hydrogen bond

View Article Online
DOI: 10.1039/C6MB00712K

acceptors (HBA), two hydrogen bond donors (HBD). As is shown in **Figure 3b**, Hypo 1 was the most desirable hypothesis due to that all the molecules in inactive testing set were appeared to be blue. Additionally, all molecules in the training set were fit to the model well, while the inactive testing set were not satisfied with the model well. Therefore, Hypo 1 was selected as the best hypothesis to go through the next research.

3.3 Pharmacophore based virtual screening

The specs database was first screened for drug like properties using Lipinski rule of 5 and Veber rule. The remaining 75671 compounds were secondly filtered through docking, and top 10000 molecules of score list were screened by Pharmacophore. Hypo 1 was used as the model to screen the potential TNKS inhibitors. As a result, the 500 compounds with top scores during the pharmacophore based virtual screening were selected for the further structural clustering analysis.

3.4 Clustering analysis

According to visual inspection, the most favorable compounds with the best binding modes binding to both Induced-pocket and nicotinamide sites were selected. Based on the knowledge of the existing TNKS inhibitors and the active site requirements, 13 compounds were selected for subsequent bioactivity prediction and consensus scoring function assay. Finally, three novel skeletons (**PYL-3**, **PYL-4, PYL-5)** exhibited a good Wnt signaling inhibition. So several their derivatives achieved by the similarity searching were used to look for some compounds with similar structure. Moreover, during our survey, another 2 compounds **PYL-1**, **PYL-2**, belong to the analogue of **PYL-3**, had also been reported as TNKS inhibitors.

3.5 Luciferase reporter assay of transcriptional activity of wnt signaling

The structures and inhibition results (IC_{50}) from Luciferase reporter assays were shown in **Table 1**. It suggested that three kinds of hits, such as three propanamides, one ethanone, one hexanamide. Among them, both propanamide and ethanone had phenyltriazole substructure, while the skeleton of hexanamide (**PYL-5**) was very

View Article Online
DOI: 10.1039/C6MB00712K

different from the others. Furthermore, the inhibition results showed that **PYL-1** was the best hits (IC50=9.56μM). IC50 values of **PYL-4** and **PYL-5** were 24.83μM and over 25μM, respectively.

3.6 SARs analysis

Combining the best pharmacophore model, docking, and consensus scoring function activity prediction, we were able to perform virtual screening on a dataset to identify potential TNKS inhibitors and to examine essential interactions responsible for binding to TNKS. Molecular docking of 5 hits was processed again with the same parameter setting by GOLD program. The interactions between the crystal structure of TNKS 2 and inhibitors were drawn by DS 4.0, SYBYL, Pymol. As is shown, the binding cave was of gourd shape, which was almost in the center of the crystal structure of TNKS 2. According to published literatures, TNKS 2 mainly consisted of two binding site[33, 39]: nicotinamide isosteres (NI) and adjacent induced pocket (IP) [40 39 38]. The XAV939 binding to NI formed hydrogen bonds with the S1068 and G1032 and formed a π-π stacking interaction with Y1071[33]. While binding of IWR-1, which belonged to IP inhibitors, showed that Y1050, Y1060 and D1045 were the key residues[33].

The interactions of three kinds of hits with the active dual sites of TNKS 2 protein were shown in **Figure 4**. In general, 5 compounds were proposed to bind with the two sites of TNKS 2. The binding modes of 5 compounds were chosen to go on with the further SARs analysis as follows.

It has been reported that some residues played vital roles in TNKS 2, such as P1034, F1035, I1039, K1042, F1044, D1045, H1048, Y1050, Y1060, E1138, I1075, S1068, Y1071, G1032.[33] In our study, **Figure 4a1-4b1**, the receptor-ligand interaction between **PYL-1** and TNKS 2, showed that **PYL-1** exhibited good biological activity because of the amino acids mentioned above involved in the interaction. In the binding pocket, **PYL-1** formed two crucial hydrogen bonds, three π-π stackings and other multiple non-bonding interactions. At the nicotinamide-binding site, as the binding mode of Olaparib,[33] **PYL-1** formed a similar close π bond with Y1071 and

View Article Online
DOI: 10.1039/C6MB00712K

generated Van Der Waals interactions with G1032, I1075, S1068. While at the adjacent induced-pocket, **PYL-1** formed two hydrogen bonds, one at the middle part with the main residue of Y1060 and the other at bottleneck part with H1048. The interactions of other two hits of propanamides were almost the same. **Figure 4a2-4b2** and **Figure 4a3-4b3** showed **PYL-2** and **PYL-3** interactions with TNKS 2, respectively. **PYL-2** bound with TNKS 2 with the same conformation as **PYL-1**, formed two hydrogen bonds and π-π stacking with the amino acids of H1048, Y1060 and Y1071. **PYL-3** generated three different hydrogen bonds with other residues, one at nicotinamide-binding site with S1068, the other two at the adjacent induced-pocket with H1031. **Figure 4a4-4b4** showed the interaction between **PYL-4** and TNKS-2, two triazole rings produced hydrogen bonds with Y1060 and F1044, π-π stacking with Y1071. Similarly, **PYL-5** formed one hydrogen bond with F1044 at the adjacent induced-pocket, and two with G1032 and S1068 at nicotinamide-binding site (**Figure 4a5-4b5**). All in all, Y1060, H1048, H1031, S1068, F1044, G1032 and S1068 were the residues involved in H-bond formation. Y1071 was the residue involved in π-π interaction. In addition, P1034, F1035, I1039, K1042, D1045, Y1050, E1138, I1075, S1068, G1032 participated in the Van Der Waals interactions. Based on the IC_{50} of five hits, one can drew conclusions that Y1060 and H1048 were the key residues by forming H-bonds at the adjacent induced-pocket. Y1071 forming π-π stacking was also vital interaction. These interactions made **PYL-1** a high affinity to TNKS 2.

4 Conclusions

In this work, a rational combination method was applied to search effective TNKS inhibitors, including molecular docking, pharmacophore model based on the known TNKS inhibitors, and Luciferase reporter assays. Consequently, 5 compounds were found for the first time to be active TNKS inhibitors. 3 propanamide analogues, 1 ethanone and 1 hexanamide showed TNKS inhibitory activity, which were then tested the inhibitory activity of Wnt signaling pathway. Among them, **PYL-1** presented the best inhibitory activity (IC_{50}=9.56μM). Furthermore, the interaction modes between TNKS and 5 compounds were disclosed through molecular docking

View Article Online
DOI: 10.1039/C6MB00712K

studies. It showed that they can bind with the structure of TNKS 2 stably through some bonding interactions and non-bonding interactions. Residues S1068, I1075, Y1071 and G1032 in the Nicotinamide isosteres site and Y1060, H1048 and Y1050 in the Induced-Pocket site were suggested to be crucial residues due to the formation of hydrogen bonds and π-π stacking with the ligands. Our results were further validated by Luciferase reporter assays. Our research would provide a foundation for the further study of dual-sites-active TNKS inhibitors and for the development of more potent Wnt signaling inhibitors.

Acknowledgements

We gratefully thank financial assistance from the Science and Technology Innovation Talent Project of Sichuan province (grant number 2016073), the State Key Laboratory of Phytochemistry and Plant Resources in West China, Kunming Institute of Botany, Chinese Academy of Sciences (grant number P2013-ZZ05), Western Light Talent Culture Project [2014]91(to Z.Z.), and Basic Research Plan of Yunnan Provincial Science and Technology Department (grant number 2014FA042).

References

1. P. Polakis, *Current Opinion in Genetics & Development*, 2007, **17**, 45-51.
2. N. Barker and H. Clevers, *Nat Rev Drug Discov*, 2006, **5**, 997-1014.
3. S.-M. A. Huang, Y. M. Mishina, S. Liu, A. Cheung, F. Stegmeier, G. A. Michaud, O. Charlat, E. Wiellette, Y. Zhang, S. Wiessner, M. Hild, X. Shi, C. J. Wilson, C. Mickanin, V. Myer, A. Fazal, R. Tomlinson, F. Serluca, W. Shao, H. Cheng, M. Shultz, C. Rau, M. Schirle, J. Schlegl, S. Ghidelli, S. Fawell, C. Lu, D. Curtis, M. W. Kirschner, C. Lengauer, P. M. Finan, J. A. Tallarico, T. Bouwmeester, J. A. Porter, A. Bauer and F. Cong, *Nature*, 2009, **461**, 614-620.
4. B. Chen, M. E. Dodge, W. Tang, J. Lu, Z. Ma, C.-W. Fan, S. Wei, W. Hao, J. Kilgore, N. S. Williams, M. G. Roth, J. F. Amatruda, C. Chen and L. Lum, *Nat Chem Biol*, 2009, **5**, 100-107.
5. S. Smith and T. de Lange, *Curr. Biol.*, 2000, **10**, 1299-1302.
6. H. Seimiya, Y. Muramatsu, T. Ohishi and T. Tsuruo, *Cancer Cell*, 2005, **7**, 25-37.
7. C. M. Counter, F. M. Botelho, P. Wang, C. B. Harley and S. Bacchetti, *Journal of Virology*, 1994, **68**, 3410-3414.
8. C. M. Counter, A. A. Avilion, C. E. LeFeuvre, N. G. Stewart, C. W. Greider, C. B. Harley and S. Bacchetti, *The EMBO Journal*, 1992, **11**, 1921-1929.
9. M. Folini, P. Gandellini and N. Zaffaroni, *Biochimica et Biophysica Acta (BBA) - Molecular*

View Article Online
DOI: 10.1039/C6MB00712K

Basis of Disease, 2009, **1792**, 309-316.

10. P. Chang, M. Coughlin and T. J. Mitchison, *Nat Cell Biol*, 2005, **7**, 1133-1139.
11. W. Chang, Jasmin N. Dynek and S. Smith, *Biochemical Journal*, 2005, **391**, 177-184.
12. P. Chang, M. Coughlin and T. J. Mitchison, *Molecular Biology of the Cell*, 2009, **20**, 4575-4585.
13. P. Kirubakaran, P. Arunkumar, K. Premkumar and K. Muthusamy, *Molecular bioSystems*, 2014, **10**, 2699-2712.
14. D.-F. Zhu, G.-L. Zhu, L.-M. Kong, N.-M. Bao, L. Zhou, Y. Nian and M.-H. Qiu, *Natural Products and Bioprospecting*, 2015, **5**, 61-67.
15. Z.-N. Ye, M.-Y. Yu, L.-M. Kong, W.-H. Wang, Y.-F. Yang, J.-Q. Liu, M.-H. Qiu and Y. Li, *Natural Products and Bioprospecting*, 2015, **5**, 91-97.
16. A. Hakmé, H.-K. Wong, F. Dantzer and V. Schreiber, *EMBO Reports*, 2008, **9**, 1094-1100.
17. M. O. Hottiger, P. O. Hassa, B. Lüscher, H. Schüler and F. Koch-Nolte, *Trends in Biochemical Sciences*, 2010, **35**, 208-219.
18. Y. J. Chiang, S. J. Hsiao, D. Yver, S. W. Cushman, L. Tessarollo, S. Smith and R. J. Hodes, *PLoS One*, 2008, **3**, e2639.
19. S. J. Hsiao and S. Smith, *Biochimie*, 2008, **90**, 83-92.
20. J. L. Riffell, C. J. Lord and A. Ashworth, *Nat Rev Drug Discov*, 2012, **11**, 923-936.
21. R. J. R. Elliott, A. Jarvis, M. B. Rajasekaran, M. Menon, L. Bowers, R. Boffey, M. Bayford, S. Firth-Clark, R. Key, R. Aqil, S. B. Kirton, D. Niculescu-Duvaz, L. Fish, F. Lopes, R. McLeary, I. Trindade, E. Vendrell, F. Munkonge, R. Porter, T. Perrior, C. Springer, A. W. Oliver, L. H. Pearl, A. Ashworth and C. J. Lord, *MedChemComm*, 2015, **6**, 1687-1692.
22. J. Roos, S. Grosch, O. Werz, P. Schroder, S. Ziegler, S. Fulda, P. Paulus, A. Urbschat, B. Kuhn, I. Maucher, J. Fettel, T. Vorup-Jensen, M. Piesche, C. Matrone, D. Steinhilber, M. J. Parnham and T. J. Maier, *Pharmacology & therapeutics*, 2016, **157**, 43-64.
23. E. Wahlberg, T. Karlberg, E. Kouznetsova, N. Markova, A. Macchiarulo, A.-G. Thorsell, E. Pol, A. Frostell, T. Ekblad, D. Oncu, B. Kull, G. M. Robertson, R. Pellicciari, H. Schuler and J. Weigelt, *Nat Biotech*, 2012, **30**, 283-288.
24. J. Waaler, O. Machon, L. Tumova, H. Dinh, V. Korinek, S. R. Wilson, J. E. Paulsen, N. M. Pedersen, T. J. Eide, O. Machonova, D. Gradl, A. Voronkov, J. P. von Kries and S. Krauss, *Cancer research*, 2012, **72**, 2822-2832.
25. B. Chen, M. E. Dodge, W. Tang, J. Lu, Z. Ma, C.-W. Fan, S. Wei, W. Hao, J. Kilgore, N. S. Williams, M. G. Roth, J. F. Amatruda, C. Chen and L. Lum, *Nature chemical biology*, 2009, **5**, 100-107.
26. H. Gunaydin, Y. Gu and X. Huang, *PLoS One*, 2012, **7**, e33740.
27. Z. Hua, H. Bregman, J. L. Buchanan, N. Chakka, A. Guzman-Perez, H. Gunaydin, X. Huang, Y. Gu, V. Berry, J. Liu, Y. Teffera, L. Huang, B. Egge, R. Emkey, E. L. Mullady, S. Schneider, P. S. Andrews, L. Acquaviva, J. Dovey, A. Mishra, J. Newcomb, D. Saffran, R. Serafino, C. A. Strathdee, S. M. Turci, M. Stanton, C. Wilson and E. F. DiMauro, *Journal of Medicinal Chemistry*, 2013, **56**, 10003-10015.
28. J. A. DiMasi, R. W. Hansen and H. G. Grabowski, *Journal of Health Economics*, 2003, **22**, 151-185.
29. N. M. Cerqueira, D. Gesto, E. F. Oliveira, D. Santos-Martins, N. F. Bras, S. F. Sousa, P. A. Fernandes and M. J. Ramos, *Archives of biochemistry and biophysics*, 2015, DOI:

View Article Online
DOI: 10.1039/C6MB00712K

10.1016/j.abb.2015.05.011.

30. M. Danishuddin and A. U. Khan, *Methods (San Diego, Calif.)*, 2015, **71**, 135-145.
31. T. Haikarainen, H. Venkannagari, M. Narwal, E. Obaji, H.-W. Lee, Y. Nkizinkiko and L. Lehtiö, *PLoS One*, 2013, **8**, e65404.
32. T. Haikarainen, M. Narwal, P. Joensuu and L. Lehtio, *ACS medicinal chemistry letters*, 2014, **5**, 18-22.
33. M. Narwal, H. Venkannagari and L. Lehtio, *J Med Chem*, 2012, **55**, 1360-1367.
34. H. Bregman, H. Gunaydin, Y. Gu, S. Schneider, C. Wilson, E. F. DiMauro and X. Huang, *J Med Chem*, 2013, **56**, 1341-1345.
35. L. L. Yang, G. B. Li, H. X. Yan, Q. Z. Sun, S. Ma, P. Ji, Z. R. Wang, S. Feng, J. Zou and S. Y. Yang, *European journal of medicinal chemistry*, 2012, **56**, 30-38.
36. C. A. Lipinski, F. Lombardo, B. W. Dominy and P. J. Feeney, *Advanced Drug Delivery Reviews*, 2001, **46**, 3-26.
37. D. F. Veber, S. R. Johnson, H. Y. Cheng, B. R. Smith, K. W. Ward and K. D. Kopple, *Journal of medicinal chemistry*, 2002, **45**, 2615-2623.
38. M. L. Verdonk, J. C. Cole, M. J. Hartshorn, C. W. Murray and R. D. Taylor, *Proteins*, 2003, **52**, 609-623.
39. P. Liscio, A. Carotti, S. Asciutti, M. Ferri, M. M. Pires, S. Valloscuro, J. Ziff, N. R. Clark, A. Macchiarulo, S. A. Aaronson, R. Pellicciari and E. Camaioni, *European journal of medicinal chemistry*, 2014, **87**, 611-623.
40. D. M. Quinn, *Chemical Reviews*, 1987, **87**, 955-979.

View Article Online
DOI: 10.1039/C6MB00712K

Novel dual sites TNKS inhibitors discovery by pharmacophore modeling, molecular docking and bioassay

Graphic Abstract

View Article Online
DOI: 10.1039/C6MB00712K

Table 1 Structures and IC_{50} values of 5 compounds against TNKS 2

Compound	STRUCTURE	Activity (SD) (IC_{50}/μM)
PYL-1	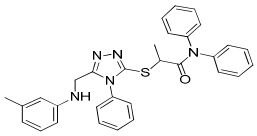	9.56
PYL-2	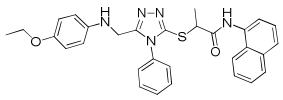	12.68
PYL-3	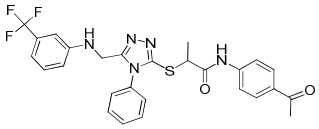	20.01
PYL-4	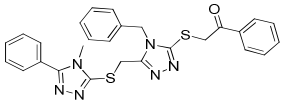	24.83
PYL-5	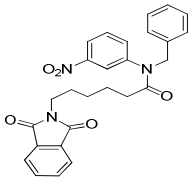	>25

View Article Online
DOI: 10.1039/C6MB00712K

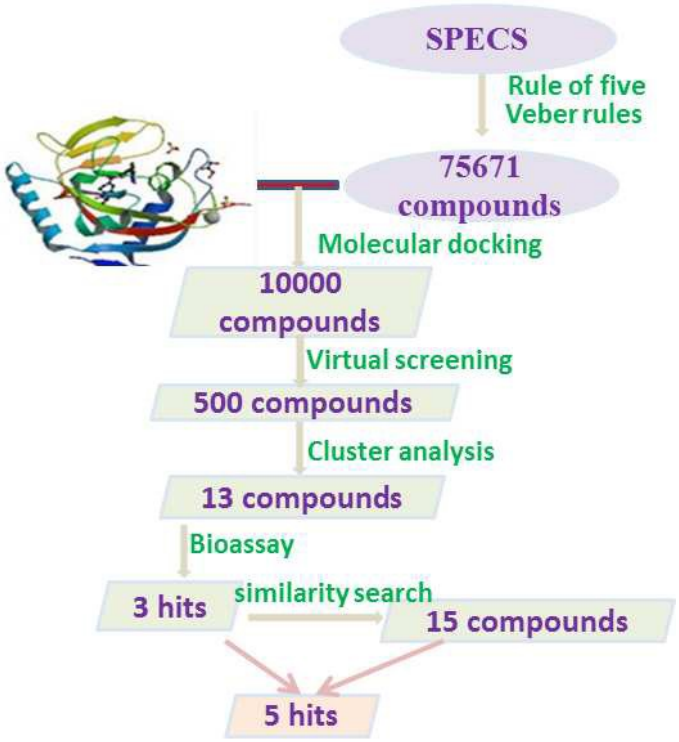

Figure 1. Overview of the workflow.

View Article Online
DOI: 10.1039/C6MB00712K

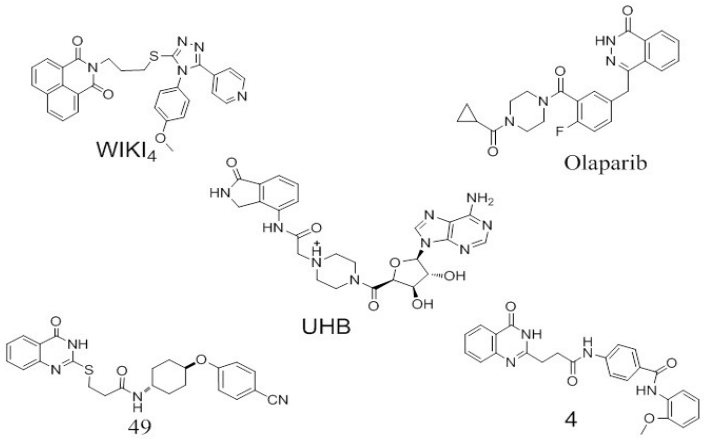

Figure 2. Chemical structures of the training set compounds.

View Article Online
DOI: 10.1039/C6MB00712K

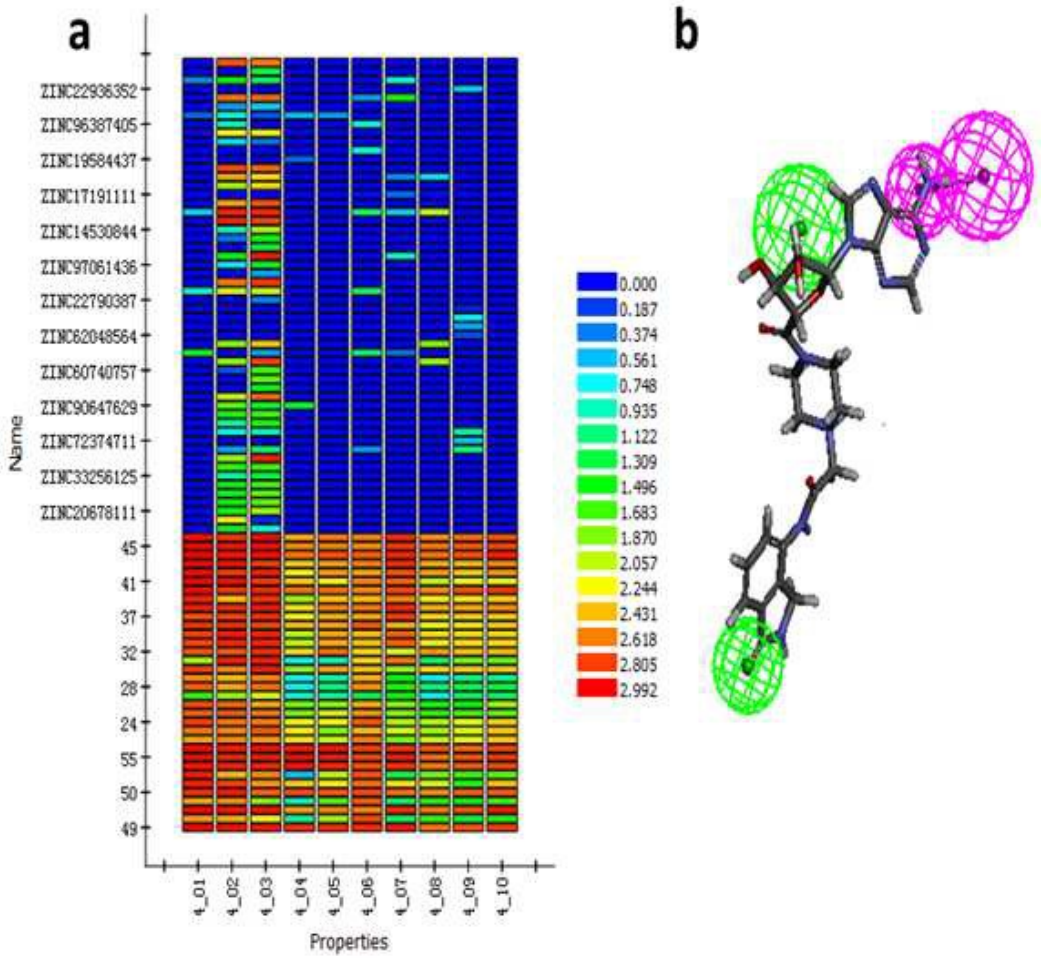

Figure 3. HipHop pharmacophore validation. **a**) heatmap of the ten hypotheses. **b**) the chemical features and 3D structure of Hypo 1 binding with UHB. Two colors represented two pharmacophore features, green represented HBA, magenta represented HBD.

View Article Online
DOI: 10.1039/C6MB00712K

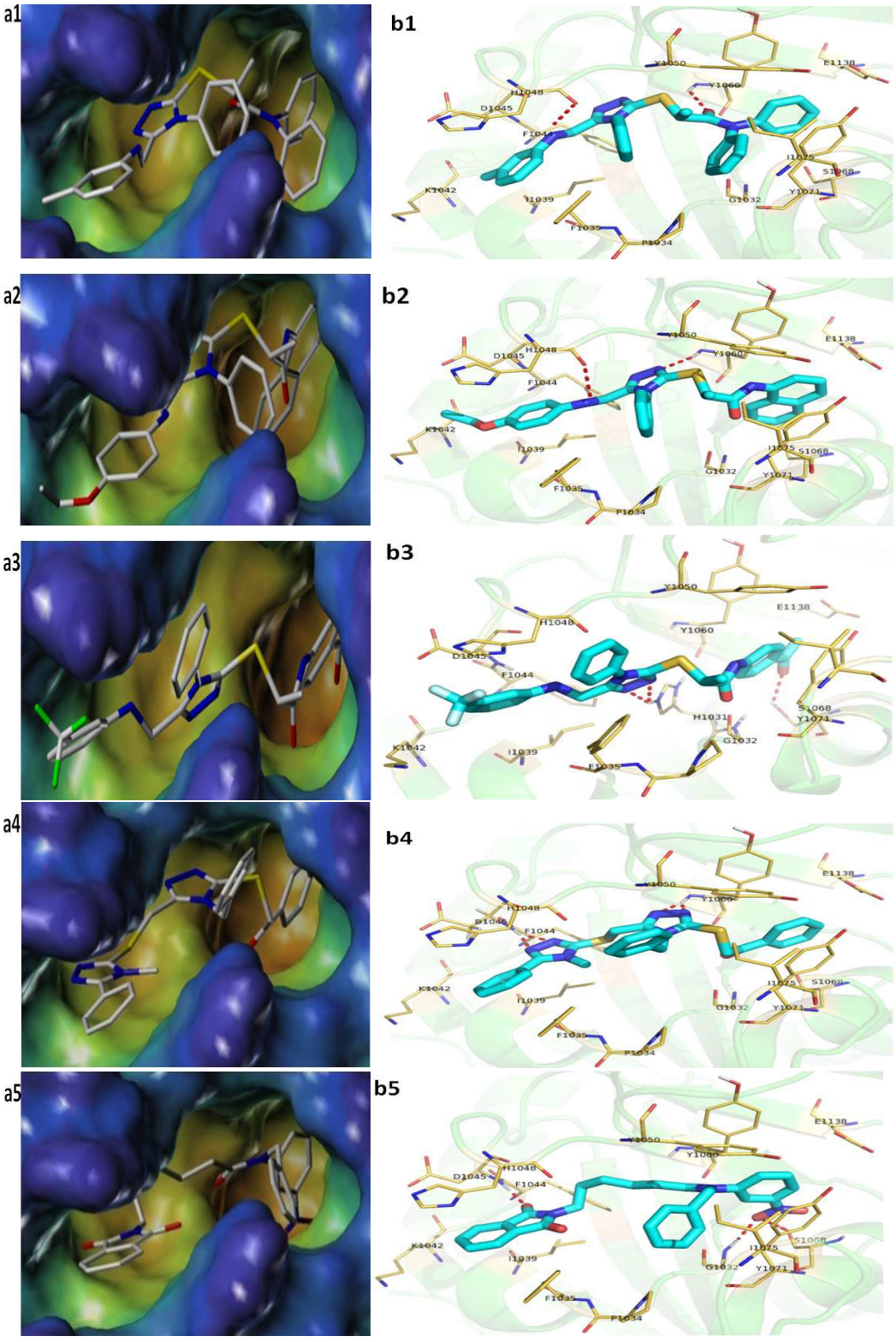

Figure 4. The receptor-ligand interaction of hits with TNKS 2. **a1, a2, a3, a4, a5**) the binding mode of **PYL-1**, **PYL-2**, **PYL-3**, **PYL-4**, **PYL-5** with TNKS 2 carried out by SYBYL. Grey sticks were represented the ligand, and blue and green

View Article Online
DOI: 10.1039/C6MB00712K

represented active cave. **b1**, **b2**, **b3**, **b4**, **b5**) the interactions between **PYL-1**, **PYL-2**, **PYL-3**, **PYL-4**, **PYL-5** and TNKS 2 carried out by Pymol. Orange sticks were represented the residues in TNKS 2, and the ligand was skyblue, red dash line represented hydrogen bonds.